JACS
JOURNAL OF THE AMERICAN CHEMICAL SOCIETY

COMMUNICATION

pubs.acs.org/JACS

Morphology and Persistence Length of Amyloid Fibrils Are Correlated to Peptide Molecular Structure

Corianne C. vandenAkker,[†] Maarten F. M. Engel,[†] Krassimir P. Velikov,[‡,§] Mischa Bonn,[†,∥] and Gijsje H. Koenderink*[,†]

[†]FOM Institute AMOLF, Science Park 104, 1098 XG, Amsterdam, The Netherlands

[‡]Unilever R&D Vlaardingen, Olivier van Noortlaan 120, 3133 AT Vlaardingen, The Netherlands

[§]Soft Condensed Matter, Debye Institute for Nanomaterials Science, Department of Physics and Astronomy, Utrecht University, Princetonplein 5, 3584 CC, Utrecht, The Netherlands

[∥]Max Planck Institute for Polymer Research, Ackermannweg 10, 55128 Mainz, Germany

Supporting Information

ABSTRACT: The formation of amyloid fibrils is a self-assembly process of peptides or proteins. The superior mechanical properties of these fibrils make them interesting for materials science but constitute a problem in amyloid-related diseases. Amyloid structures tend to be polymorphic, and their structure depends on growth conditions. To understand and control the assembly process, insights into the relation between the mechanical properties and molecular structure are essential. We prepared long, straight as well as short, worm-like β-lactoglobulin amyloid fibrils and determined their morphology and persistence length by atomic force microscopy (AFM) and the molecular conformation using vibrational sum-frequency generation (VSFG) spectroscopy. We show that long fibrils with near-100% β-sheet content have a 40-times higher persistence length than short, worm-like fibrils with β-sheet contents below 80%.

Many proteins and peptides of diverse sequence, structure, and function spontaneously self-assemble into amyloid-like nanofibrils under a variety of conditions. Such fibrils are found in protein deposits of patients suffering from amyloid-related diseases, including Alzheimer's disease and type II diabetes mellitus.[1] However, the unique chemical and mechanical properties of these fibrils could also be exploited in novel biomaterials.[2] To understand and control amyloid fibril assembly, it is crucial to understand the relation between mechanical properties and molecular structure. Here we show that a distinct correlation exists between amyloid molecular structure and the structural and mechanical properties: long, straight amyloid fibrils with high persistence lengths are characterized by a high β-sheet content. In contrast, short, worm-like fibrils have a 40-times lower persistence length and drastically reduced β-sheet content.

Amyloid-like fibrils are characterized by a universal cross-β structure, in which the peptide backbone is orthogonal to the fibril axis.[3,4] Hydrogen bonds stabilize this structure and cause a high mechanical rigidity.[5] The fibrils are generally a few nanometers in diameter, reaching up to several micrometers in length, and tend to be polymorphic. For example, thin fibrils, twisted ribbons, and crystalline-like materials have been observed.[6] Aggregates of misfolded proteins were originally discovered through their involvement in Alzheimer's disease. Currently, over 20 protein conformational diseases have been identified, including Creutzfeldt-Jakob disease and type II diabetes mellitus.[1] However, amyloids also perform functional biological roles, for instance, to reinforce and structure bacterial biofilms and eggshells of fish and insects.[7−9] Amyloid fibrils are potentially interesting biomaterials, because of their high mechanical, thermal, and chemical stability. The fibrils can be easily functionalized since synthetic peptides with different primary sequences can be used. First applications that have been explored include fibrils as templates for nanowires[10] and as scaffolds for cell culture[11] or controlled drug release.[12]

Despite the apparent importance of this class of materials, it has been challenging to relate the molecular structure to fibril morphology. While the molecular pathways of fibril formation have recently been elucidated,[13,14] knowledge of the relation between the mechanical properties and molecular structure has been lagging. This is relevant for both applications in novel functional materials and disease-related amyloids. Fiber rigidity (directly related to persistence length) affects the degree to which fibers tangle to form insoluble plaques, which are a major pathological factor in systemic amyloidosis.[15] Further, a higher stiffness has been suggested to promote the disruption of cellular membranes by amyloid fibrils[16] and the mechanical rigidity influences fragmentation, which plays a major role in the kinetics of fibril growth.[5]

The model protein β-lactoglobulin (β-lg) forms amyloid fibrils upon incubation at low pH and high temperature.[17−22] We prepared β-lg amyloid fibrils of various morphologies by varying the protein concentration between 3.0 and 7.5% and the incubation time between 16 and 96 h (Supporting Information (SI) Methods). The conversion of monomers to fibrils levels off after 24 h of incubation (SI Figure 1). We studied the morphology and mechanics of amyloid fibrils by atomic force microscopy (AFM) and their molecular conformation by vibrational sum-frequency generation (VSFG) spectroscopy. The strength of combining these techniques is that identical samples can be studied: the same substrate and sample preparation can be used

Received: July 13, 2011
Published: October 14, 2011

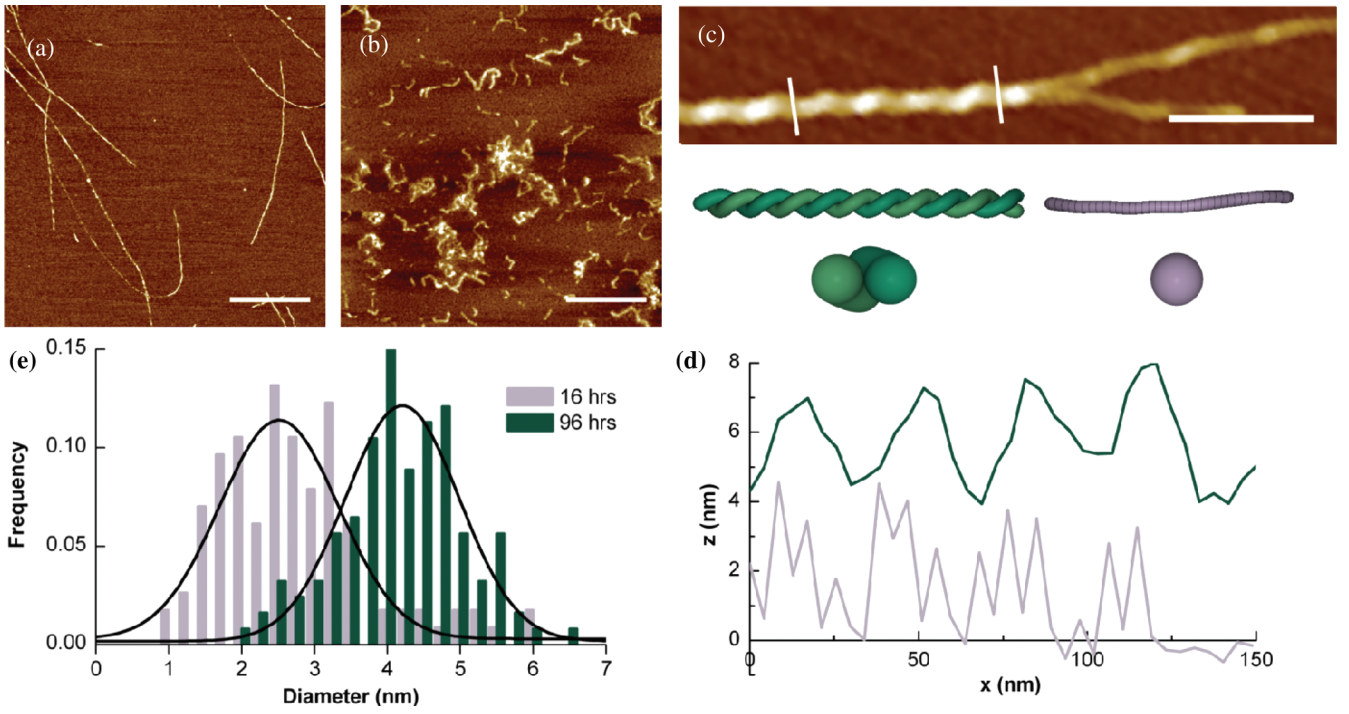

Figure 1. (a and b) AFM height images of amyloid fibrils prepared in 16 h at (a) 3.0% and (b) 7.5% β-lg. Scale bar is 500 nm. (c) A split fibril imaged using AFM in liquid and reconstructions of left-handed helical fibril formation from the twisting of a two-stranded ribbon (left) and a protofibril (right).[17] The white lines indicate fibril sections used for periodicity measurements. Scale bar is 100 nm. (d) Cross sections of the fibril shown in (c), showing periodicities of 36 nm for the helical fibril (top) and 10 nm for the protofibril (bottom). (e) Diameter distribution of fibrils formed at 3.0% β-lg during incubation times of 16 and 96 h. Black lines are Gaussian fits.

for both AFM and VSFG. AFM gives morphological information about the fiber length, diameter, and shape, from which the persistence length can be quantified.[22,23] VSFG provides information on the secondary structure and orientation of materials at surfaces or interfaces.[24] It utilizes two pulsed laser beams: one at visible and one at infrared (IR) frequency. As a result of interaction with the molecules at the surface, light at the sum frequency of the visible and IR beams is generated. When the IR frequency matches a surface vibrational mode frequency, this process may be resonantly enhanced. Conformations of proteins are investigated by probing the amide I region (1600−1700 cm^{-1}), where β-sheets characteristic of amyloids can be distinguished from structures such as random coils and α-helices.[25] VSFG spectroscopy is a sensitive, label-free method that so far has been rarely used to determine the secondary structure of amyloids.[26,27]

To assess the morphology of the amyloid fibrils, we used tapping mode AFM (SI Methods). The contour length distributions reveal that long, straight fibrils show a broad length distribution, spanning a range of 0.2 μm up to 5 μm, whereas the worm-like fibrils have much shorter lengths (between 0.1 and 0.5 μm) (Figure 1a and b, SI Table 1). The short fibril length may be a consequence of the formation of more nuclei and therefore more fibrils at high concentrations of β-lg. At lower β-lg concentrations, the elongation rate probably dominates over the nucleation rate, and very long fibrils are formed. The short, worm-like fibrils are reminiscent of previously observed fibrils formed at high ionic strength or in water-ethanol mixtures.[18,28]

We measured the height profiles of β-lg fibrils using AFM. The height profiles showed a periodicity of ∼10 nm for thin fibrils (presumably protofibrils) and a periodicity of ∼36 nm for fibrils composed of two protofibrils (Figure 1c and d). These observations are in agreement with previously reported periodicities of β-lg fibrils.[19] We quantified the diameter of the fibrils from their maximum height. As shown in Figure 1e and SI Table 1, long, straight fibrils have an average diameter of about 2.6 nm after 16 h of incubation. The diameter distribution is rather broad, with a main population in the range of 1−3.5 nm, and a tail with thicker fibrils having diameters of 4−6 nm. This observation is consistent with prior AFM studies of β-lg fibrils formed in 24 h, which also displayed different populations of fibrils with distinct diameters.[19] After 96 h of incubation, the diameter distribution is narrower and shifted to larger diameter values. The average diameter is now almost 2-fold higher than that after 16 h of incubation, amounting to ∼4 nm. Our interpretation is that single protofibrils are predominantly formed for incubation times up to 16 h. Thicker fibrils composed of two or more protofibrils are formed after longer incubation times. As shown in SI Table 1, the same influence of incubation time on the fibril diameter is seen at other β-lg concentrations. The β-lg concentration itself does not strongly influence the fibril diameter.

We measured the persistence length from the shape of the fibrils, more specifically from the relation between their contour length, C, and end-to-end distance, E (SI Methods).[29,30] To calculate the persistence length, E^2 was plotted as a function of C. Figure 2 shows experimental data with theoretical fits for long, straight and short, worm-like fibrils formed in 16 h. There was a clear distinction between the straight fibrils formed at a protein concentration of 3.0% and the worm-like fibrils formed at 7.5% (SI Table 1). The straight fibrils have persistence lengths around

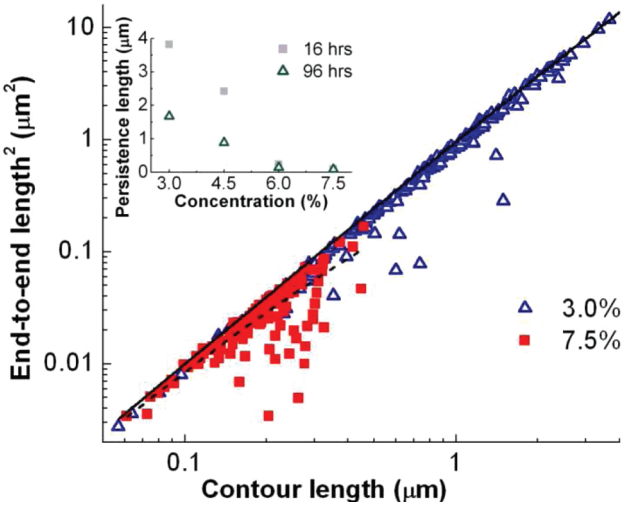

Figure 2. Plot of the squared end-to-end distance versus contour length for fibrils formed at 3.0 and 7.5% β-lg in 16 h (symbols) and corresponding fits (solid line: 3.0%; dashed line: 7.5%). Inset: Persistence lengths of fibrils formed at concentrations of 3.0 to 7.5% β-lg in 16 and 96 h.

3818 ± 164 nm, while the worm-like fibrils have a persistence length of only 92 ± 7 nm, consistent with previous findings.[31−33] The persistence length decreases for increasing β-lg concentration.

The observation of two distinct fibril morphologies by AFM raises the question whether the secondary structure of these fibril types is different. To measure the secondary structure content, we acquired VSFG spectra in the amide I region. Figure 3a presents the amide I spectra for amyloid fibrils formed at concentrations between 3.0 and 7.5% β-lg in 16 h. For the long, straight fibrils formed at 3.0% β-lg, the amide I bands are centered at ∼1625 cm^{-1}, which is assigned to β-sheet structure.[34,35] In contrast, the peak position shifts to higher wavenumbers for worm-like fibrils formed at 7.5% β-lg. To analyze the secondary structures of β-lg fibrils, the spectra were fitted using a two-component Lorentzian model. The components center in two regimes: 1620−1643 cm^{-1}, which is assigned to β-sheets, and 1643−1666 cm^{-1}, which is assigned to disordered structures and/or α-helices.[25,34−36] We calculated the fraction of the integrated intensity of peaks fitted to the VSFG data for these two bands (Figure 3b). In our analysis we have assumed that the transition dipole and the Raman dipole are the same for the different types of secondary structure, similar to prior studies.[26,27] Although this is not strictly true,[36−38] a detailed analysis taking into account the IR and Raman transition dipoles would be extremely difficult due to the complexity (i.e., size distribution, unknown concentration) of the amyloid fibril samples that we use in our study. In addition, the AFM data show that the fibrils are randomly oriented on the surface, thereby canceling any orientation dependency in the SFG intensity.

The β-sheet intensity is close to 100% for 3.0% β-lg but drops to approximately 40% when increasing the β-lg concentration to 7.5% for samples incubated for 16 h (Figure 3). For samples incubated for 96 h, the β-sheet intensity also drops, from close to 100% to 55% (SI Figure 5). The fits and the fit parameters for each spectrum are shown in SI Figures 3 and 4 and in SI Table 2.

The straight and worm-like fibrils therefore not only possess a different morphology but also a fundamentally different secondary structure. Worm-like fibrils formed at high β-lg

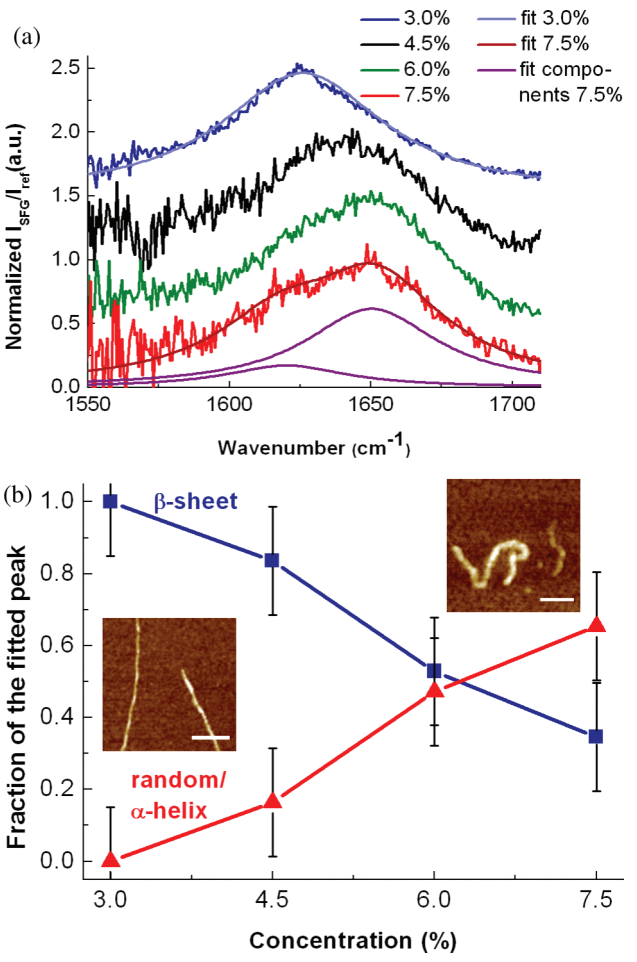

Figure 3. (a) Normalized VSFG spectra and (b) fraction of β-sheet and random/α-helical intensity of fibrils formed at concentrations of 3.0 to 7.5% β-lg in 16 h. Spectra and fractions are averages from three measurements. Spectra have been normalized and are plotted with an offset of 0.5 au along the y-axis. Scale bar in AFM images is 100 nm.

concentrations mainly consist of unordered and/or α-helical structures, whereas straight fibrils are composed of β-sheets. The β-sheet-rich long, straight fibrils have a 40 times higher persistence length compared to the short, worm-like fibrils. The high persistence length likely originates from a strong hydrogen-bonding network in the aligned backbones of the β-sheet-rich fibrils. In contrast, the much lower persistence length of the worm-like fibrils suggests that weaker intermolecular forces are present, as is expected for the less-organized fibrils with reduced β-sheet content that we observe here. Moreover, there may be structural defects in the fibril backbone leading to intrinsic curvature. These notions agree with the recent suggestion of a positive correlation between β-sheet structure and persistence length.[5]

The combined use of AFM and VSFG spectroscopy provides morphological, mechanical, and structural information of amyloid fibrils deposited on a solid surface. We show that short, worm-like fibrils formed at high β-lg concentrations contain less β-sheet content than long, straight fibrils. This can be related to the lower persistence length that is observed. The negative correlation between monomer concentration on the one hand, and β-sheet content, fibril length, and persistence length on the other, is presumably related to the formation of more nuclei, and more (proto-)fibrils at high concentration, which then assemble

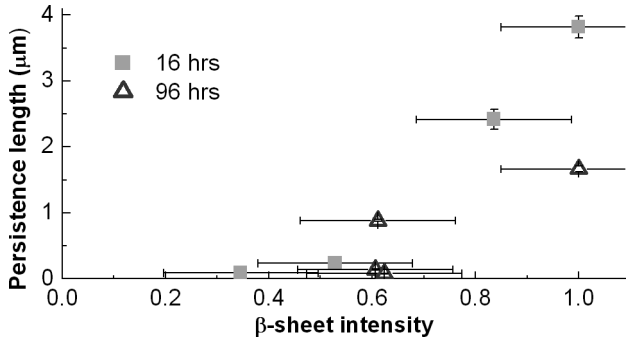

Figure 4. Plot of the persistence length versus the intensity of β-sheet content of fibrils formed at concentrations of 3.0 to 7.5% β-lg in 16 and 96 h.

into more disordered structures. Correlating β-sheet content and persistence length suggests that a substantial increase in persistence length can only be achieved at β-sheet contents near 100% (Figure 4). These results may aid the future, rational design of nanobiomaterials with specific mechanical properties.

■ ASSOCIATED CONTENT

Supporting Information. Experimental procedures and supporting figures and tables are included in the Supporting Information. This material is available free of charge via the Internet at http://pubs.acs.org.

■ AUTHOR INFORMATION

Corresponding Author
g.koenderink@amolf.nl

■ ACKNOWLEDGMENT

The authors thank N. Mücke for help with persistence length calculations. This work is part of the Industrial Partnership Programme (IPP) Bio(-Related) Materials (BRM) of the Stichting voor Fundamenteel Onderzoek der Materie (FOM), which is financially supported by the Nederlandse Organisatie voor Wetenschappelijk Onderzoek (NWO). The IPP BRM is cofinanced by the Top Institute Food and Nutrition and the Dutch Polymer Institute.

■ REFERENCES

(1) Stefani, M.; Dobson, C. M. *J. Mol. Med.* **2003**, *81*, 678–699.
(2) Cherny, I.; Gazit, E. *Angew. Chem., Int. Ed.* **2008**, *47*, 4062–4069.
(3) Krebs, M. R. H.; Domike, K. R.; Cannon, D.; Donald, A. M. *Faraday Discuss.* **2008**, *139*, 265–274.
(4) Tycko, R. *Curr. Opin. Struct. Biol.* **2004**, *14*, 96–103.
(5) Knowles, T. P.; Fitzpatrick, A. W.; Meehan, S.; Mott, H. R.; Vendruscolo, M.; Dobson, C. M.; Welland, M. E. *Science* **2007**, *318*, 1900–1903.
(6) Marshall, K. E.; Serpell, L. C. *Soft Matter* **2010**, *6*, 2110–2114.
(7) Fowler, D. M.; Koulov, A. V.; Balch, W. E.; Kelly, J. W. *Trends Biochem. Sci.* **2007**, *32*, 217–224.
(8) Chiti, F.; Dobson, C. M. *Annu. Rev. Biochem.* **2006**, *75*, 333–366.
(9) Otzen, D.; Nielsen, P. H. *Cell. Mol. Life Sci.* **2008**, *65*, 910–927.
(10) Scheibel, T.; Parthasarathy, R.; Sawicki, G.; Lin, X. M.; Jaeger, H.; Lindquist, S. L. *Proc. Natl. Acad. Sci. U.S.A.* **2003**, *100*, 4527–4532.
(11) Gelain, F.; Bottai, D.; Vescovi, A.; Zhang, S. G. *PLoS One* **2006**, *1*, e119.
(12) Maji, S. K.; Schubert, D.; Rivier, C.; Lee, S.; Rivier, J. E.; Riek, R. *PLoS Biol.* **2008**, *6*, 240–252.
(13) Shim, S. H.; Gupta, R.; Ling, Y. L.; Strasfeld, D. B.; Raleigh, D. P.; Zanni, M. T. *Proc. Natl. Acad. Sci. U.S.A.* **2009**, *106*, 6614–6619.
(14) Knowles, T. P. J.; Shu, W.; Devlin, G. L.; Meehan, S.; Auer, S.; Dobson, C. M.; Welland, M. E. *Proc. Natl. Acad. Sci. U.S.A.* **2007**, *104*, 10016–10021.
(15) Tan, S. Y.; Pepys, M. B. *Histopathology* **1994**, *25*, 403–414.
(16) Engel, M. F. M.; Khemtemourian, L.; Kleijer, C. C.; Meeldijk, H. J. D.; Jacobs, J.; Verkleij, A. J.; de Kruijff, B.; Killian, J. A.; Höppener, J. W. M. *Proc. Natl. Acad. Sci. U.S.A.* **2008**, *105*, 6033–6038.
(17) van der Linden, E.; Venema, P. *Curr. Opin. Colloid Interface Sci.* **2007**, *12*, 158–165.
(18) Gosal, W. S.; Clark, A. H.; Ross-Murphy, S. B. *Biomacromolecules* **2004**, *5*, 2408–2419.
(19) Adamcik, J.; Jung, J. M.; Flakowski, J.; De Los Rios, P.; Dietler, G.; Mezzenga, R. *Nat. Nanotechnol.* **2010**, *5*, 423–428.
(20) Arnaudov, L. N.; de Vries, R.; Ippel, H.; van Mierlo, C. P. M. *Biomacromolecules* **2003**, *4*, 1614–1622.
(21) Akkermans, C.; Venema, P.; van der Goot, A. J.; Gruppen, H.; Bakx, E. J.; Boom, R. M.; van der Linden, E. *Biomacromolecules* **2008**, *9*, 1474–1479.
(22) Gosal, W. S.; Morten, I. J.; Hewitt, E. W.; Smith, D. A.; Thomson, N. H.; Radford, S. E. *J. Mol. Biol.* **2005**, *351*, 850–864.
(23) Rivetti, C.; Guthold, M.; Bustamante, C. *J. Mol. Biol.* **1996**, *264*, 919–932.
(24) Sovago, M.; Vartiainen, E.; Bonn, M. *J. Phys. Chem. C* **2009**, *113*, 6100–6106.
(25) Chen, X. Y.; Clarke, M. L.; Wang, J.; Chen, Z. *Int. J. Mod. Phys. B* **2005**, *19*, 691–713.
(26) Fu, L.; Ma, G.; Yan, E. C. Y. *J. Am. Chem. Soc.* **2010**, *132*, 5405–5412.
(27) Fu, L.; Liu, J.; Yan, E. C. Y. *J. Am. Chem. Soc.* **2011**, *133*, 8094–8097.
(28) Arnaudov, L. N.; de Vries, R. *Biomacromolecules* **2006**, *7*, 3490–3498.
(29) Mucke, N.; Klenin, K.; Kirmse, R.; Bussiek, M.; Herrmann, H.; Hafner, M.; Langowski, J. *PLoS One* **2009**, *4*, e7756.
(30) Relini, A.; Torrassa, S.; Ferrando, R.; Rolandi, R.; Campioni, S.; Chiti, F.; Gliozzi, A. *Biophys. J.* **2010**, *98*, 1277–1284.
(31) Jordens, S.; Adamcik, J.; Amar-Yuli, I.; Mezzenga, R. *Biomacromolecules* **2011**, *12*, 187–193.
(32) Aymard, P.; Nicolai, T.; Durand, D.; Clack, A. *Macromolecules* **1999**, *32*, 2542–2552.
(33) Sagis, L. M. C.; Veerman, C.; van der Linden, E. *Langmuir* **2004**, *20*, 924–927.
(34) Tamm, L. K.; Tatulian, S. A. *Q. Rev. Biophys.* **1997**, *30*, 365–429.
(35) Oboroceanu, D.; Wang, L. Z.; Brodkorb, A.; Magner, E.; Auty, M. A. E. *J. Agric. Food Chem.* **2010**, *58*, 3667–3673.
(36) Nguyen, K. T.; King, J. T.; Chen, Z. *J. Phys. Chem. B* **2010**, *114*, 8291–8300.
(37) Nguyen, K. T.; Le Chair, S. V.; Ye, S.; Chen, Z. *J. Phys. Chem. B* **2009**, *113*, 12169–12180.
(38) Ha, S.; Kim, S.-S.; Lee, C.; Cho, M. *J. Chem. Phys.* **2005**, *123*, 084905.